Meson Production and Spectroscopy at HERA *

Jan Olsson

DESY, Notkestraße 85, 22607 Hamburg, BRD
E-mail: jan.olsson@desy.de

On behalf of the H1 and ZEUS collaborations

Selected recent results from the H1 and ZEUS experiments are reviewed, illustrating some of the many facets of "meson physics" at the HERA *ep* collider. The results cover exclusive elastic and proton-dissociative diffractive vector meson production and comparisons with recent theoretical calculations show that perturbative QCD models are successful in describing these processes when at least one of the involved scales have large values. Furthermore a search for odderon induced exclusive photoproduction of pseudoscalar and tensor mesons is described; upper limits for the cross sections are below recent theoretical predictions. Finally the status of open charm meson spectroscopy in inclusive final states is reported.

PACS numbers: 13.60.Le, 25.20.Lj

1. Introduction

In the very successful first running period, which ended in 2000, the ep collider HERA at DESY yielded more than 100 pb^{-1} of integrated luminosity for each of the two experiments H1 and ZEUS. These data provide high statistics samples in many interesting areas of physics. In the present report, recent results in three such areas, all related to "meson" physics, are described. More precisely, the topics of Exclusive Vector Meson Production, Production of Pseudoscalar and Tensor Mesons via Odderon Exchange, and finally Charm Spectroscopy, are addressed.

2. Exclusive Vector Meson Production

The diffractive, exclusive vector meson production process,

$$ep \to \ eVY, \quad \text{with } V = \quad \rho^{\circ}, \omega, \phi, J/\Psi, \Psi', \Upsilon, \tag{1}$$

* Presented at the MESON2002 Conference 24-28.5.2002, Kraków, Poland

and with Y being either a proton (elastic scattering) or a low mass hadronic system (proton dissociative scattering), has been extensively studied at HERA. Detailed reviews are given in [1, 2]. The renewed interest in this seemingly simple reaction stems from the fact that the HERA colliding beam experiments greatly extend the accessible range both of the center of mass energy and of the physics scales which are involved in the process. Thus detailed studies are possible both in the soft, low energy regime already explored by the fixed target experiments, and in the new regime, where scales reach values large enough for perturbative QCD (pQCD) to be applied, *i.e.* where Λ_{QCD} is small in comparison.

Reaction (1) is shown schematically in Fig. 1a. The virtual photon, emitted by the scattered electron, scatters diffractively off the proton to form a vector meson. The following quantities will be used in the discussion:

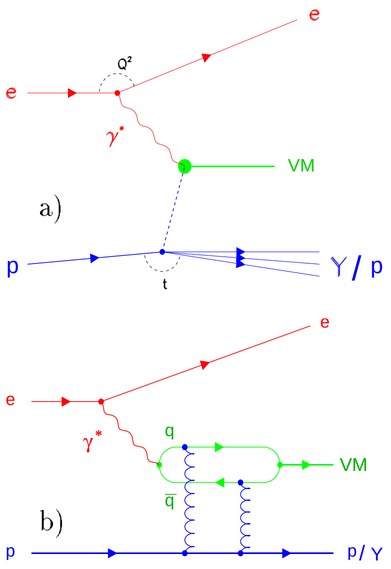

Figure 1: Exclusive vector meson production: a) schematic diagram, b) pQCD approach.

- Q^2: The photon virtuality, i.e. the absolute value of the squared 4-momentum transfer at the electron vertex (the generic term 'electron' is used for both e^+ and e^-). In the results presented here Q^2 ranges from ~ 0 to ~ 100 GeV^2.
- $W_{\gamma p}$, or simply W: the CM energy of the $\gamma^* p$ system, here in the range $20 \lesssim W_{\gamma p} \lesssim 290$ GeV.
- t: The squared 4-momentum transfer at the proton vertex, with $0 \lesssim |t| \lesssim 20$ GeV^2 in the present results. For small values of Q^2, $|t|$ is well approximated by the squared transverse momentum of the produced vector meson V, $t \approx -p_{t,V}^2$.

The classical approach, based on Regge theory and Vector Meson Dominance (VDM), gives a successful description of process (1) for the light vector mesons and for low values of Q^2 and $|t|$. Diffractive scattering means exchange of the vacuum quantum numbers, and the corresponding Regge trajectory is the Pomeron. Predictions in this approach are, among others: a slow rise of the cross section with W, *i.e.* $\sigma \propto W^{0.2-0.3}$, shrinkage of the diffractive peak with increasing W, *i.e.* $d\sigma/dt \propto e^{bt}\,(W/W_0)^{4(\alpha_{I\!P}(t)-1)}$ with

$\alpha_{I\!P}(t) = \alpha_{I\!P}(0) + \alpha'_{I\!P}\, t$ and $b = b_0 + 4\,\alpha'_{I\!P}\, ln(W/W_0)$, conservation of the S-channel helicity (SCHC) and a Q^2-dependence $\sigma \propto 1/(Q^2 + M_V^2)^2$.
In the pQCD approach, Fig. 1b, the process (1) is seen as a series of steps, well separated by the very different timescales involved (factorization):

- The virtual photon fluctuates into a $q\bar{q}$ pair, *i.e.* into a colour dipole.
- The $q\bar{q}$ pair scatters off the proton, in leading order under exchange of a pair of gluons in a colour singlet state.
- The scattered $q\bar{q}$ pair forms a bound state, the vector meson.

While the $q\bar{q}$ scattering can be described within pQCD, the $\gamma \rightarrow q\bar{q}$ and $q\bar{q} \rightarrow V$ processes are modelled with the respective wave-functions. In this approach, the cross section for (1) is proportional to the square of the gluon density $g(x, Q^2)$ in the proton[3],

$$\sigma \propto \alpha_s^2(Q^2)/Q^6\ [xg(x, Q^2)]^2, \quad (2)$$

where x is the Bjorken x. pQCD predictions for reaction (1) are partly different from those of the Regge and VDM approach. Thus the cross section will rise steeply with W, due to the increasing gluon density in the proton at small values of x and the relation $xW_{\gamma p}^2 \approx Q^2$, valid for small x at a given Q^2. Furthermore, much reduced shrinkage of the diffractive peak is expected, and SCHC is violated. The Q^2-dependence in (2) is discussed below.
The HERA data have been extensively used to demonstrate the validity of the pQCD approach, as the following examples illustrate.

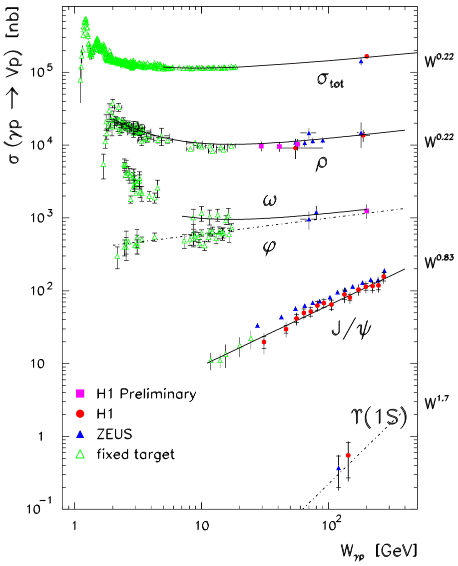

Figure 2: Compilation of cross sections for exclusive photoproduction of the vector mesons $\rho°, \omega, \phi, J/\Psi$ and Υ, as functions of $W_{\gamma p}$. Full curves represent fits using Regge parametrizations and single pomeron exchange. Dashed lines indicate $W_{\gamma p}$-dependences as given on the right hand side.

***W*-dependence of the cross sections:** Fig. 2 shows a compilation of cross section measurements $\sigma_{\gamma p \rightarrow Vp}$ vs. W, for exclusive photoproduction of vector mesons at HERA and at lower (fixed target) CM energies. Also the total photoproduction cross section is shown. The slow rise with W, as predicted in the Regge approach, is clearly seen for the light vector mesons ρ, ω and ϕ (and also for the total cross section). However, the rise with W is much steeper for the heavier J/Ψ. The observed W^{δ}-dependence can easily be related to the increasing proton gluon density at small x values: using Ryskin's [4] proposed scale $\mu^2 = (Q^2 + M^2_{J/\Psi})/4$ for photoproduction at small $|t|$, a value $\mu^2 = 2.4$ GeV^2 is obtained. At this scale, and at small x, the gluon density rises [5] as $xg(x) \propto x^{-0.2}$, thus corresponding to $\sigma \propto W^{0.8}$, which is in good agreement with the observed $\delta \sim 0.7 - 0.8$. This indicates that the mass of the c-quark can be used as a hard scale in pQCD calculations. However, theory uncertainties currently limit the access to the proton gluon density via precise measurements of the W-dependence of the cross section for exclusive heavy vector meson production.

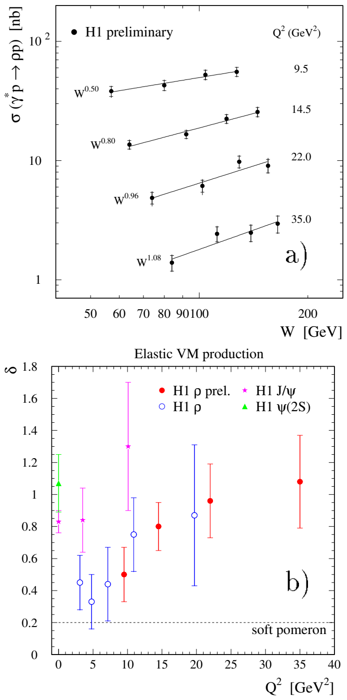

Figure 3: a) Cross section for exclusive ρ° production, as function of W for several values of Q^2. Curves show fits to the form W^{δ}. b) Values of δ vs. Q^2, for $\rho^{\circ}, J/\Psi$ and Ψ'. The dotted line shows the "soft pomeron" expectation.

What happens to the W-dependence of the cross section for light vector mesons, if another scale, *e.g.* Q^2, is increased? This is illustrated in Fig. 3a, where the cross section for $\gamma^* p \to \rho^{\circ} p$ is shown vs. W, for increasing average values of Q^2[6]. The cross section steepens in W with increasing Q^2, and soon deviates significantly from the "soft pomeron"[7] expectation, as seen in Fig. 3b where the power δ from the W^{δ} fits is plotted vs. Q^2. At $Q^2 > 10$ GeV^2 the values of δ for the ρ° cross section are the same as for the J/Ψ (or Ψ') cross section at $Q^2 \sim 0$.

The W-dependence of the J/Ψ cross section, for increasing Q^2, is shown in Fig. 4a[8]. There is no significant change when going to higher Q^2 values, the already "hard" behaviour at $Q^2 \sim 0$ does not become still harder. The data are well described by the pQCD calculations[9, 10], using recent proton parton density parametrizations[11].

The W-dependence of the J/Ψ cross section also does not change when the other scale, $|t|$, increases in value. This is seen in Fig. 4b, where the cross section is plotted vs. W for two intervals of $|t|$[12]. The pQCD model calculation in Fig. 4b[13] agrees with the data.

Q^2-dependence of the cross section: The cross section (2) contains the factor $1/Q^6$, which is much steeper than the classical, VDM expectation $1/(Q^2 + M_V^2)^2$. However, the $1/Q^6$ dependence in (2) is modified by the Q^2-dependence in α_s and in the proton gluon density. Effectively, a $1/Q^n$ dependence is predicted, with $n \approx 4-5$, depending on the Q^2 range. This is also borne out in the data. Fig. 5a shows the Q^2-dependence of the ρ° cross section with a fit to the form $1/(Q^2 + M_{\rho^\circ}^2)^n$, with $n = 2.60$ in the chosen fit interval[6]. It is clear that the whole spectrum cannot be fitted with one simple curve of this form, and that at low values of Q^2 the dependence is less steep.

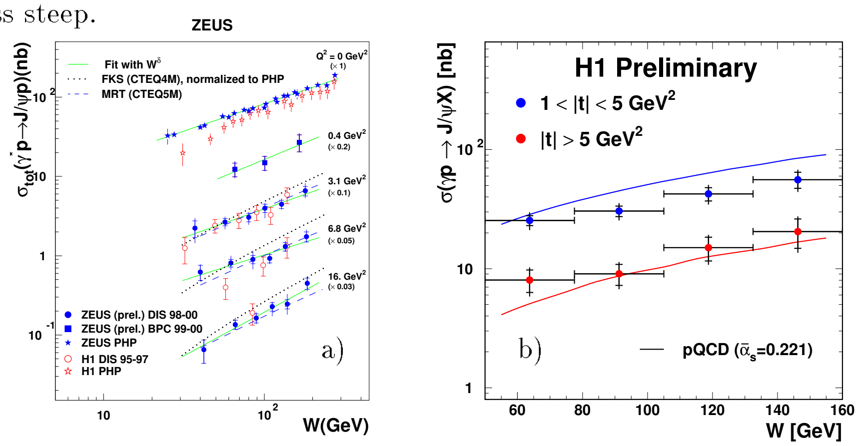

Figure 4: Cross section for exclusive J/Ψ production, as a function of W. a) For several values of Q^2. Curves show fits to the form W^δ as well as two pQCD calculations[9, 10]. b) Photoproduction, for two intervals of $|t|$. The curves show a pQCD calculation[13].

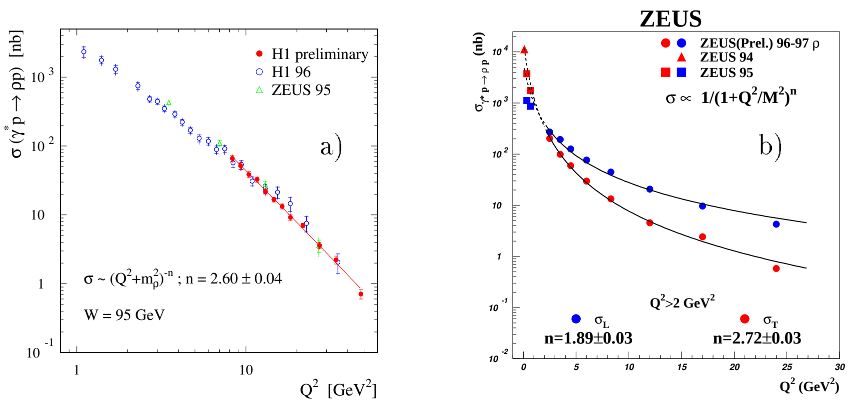

Figure 5: Q^2 dependence of the cross section for exclusive ρ° production. In a) the total ρ° cross section is shown, in b) σ_L and σ_T are shown separately.

Expression (2) is only valid for the longitudinal part of the cross section, σ_L. In [3] also the transverse part, σ_T, is calculated and predicted to have a still steeper Q^2-dependence, by another factor $1/Q^2$. Thus σ_L is expected to dominate at larger Q^2-values. Data confirm this prediction; in Fig. 5b the Q^2-dependences of σ_L and σ_T are shown separately[14]. Indeed, the Q^2-dependence of σ_L is even harder than the VDM expectation ($n = 2$).
The steepness of the Q^2-dependence of the cross section is also modified by *e.g.* the Fermi motion of the quarks [3, 15] and the suggestion has been made that, beyond the pQCD tests, precise measurements of the Q^2-dependence of the cross section for elastic vector meson electroproduction can reveal information also about the wave functions of the vector mesons.

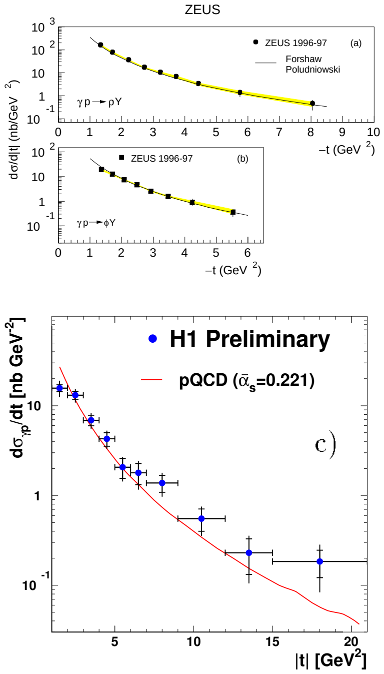

Figure 6: t-dependence of exclusive ρ° and ϕ (a-b) and J/Ψ (c) photoproduction cross sections. Curves show the pQCD models [18] (a-b) and [13] (c).

t-dependence of the cross section: New measurements[12, 16] from ZEUS and H1 of the t-dependence at large $|t|$ of the exclusive vector meson production cross section are shown in Fig. 6 for ρ°, ϕ and J/Ψ. pQCD calculations for the light vector mesons[17] predict a dependence $d\sigma/dt \propto |t|^{-n}$, n taking values from $\sim$3.8 to $\sim$4.8. Data however exhibit a flatter behaviour. The curves in Figs.6a and 6b show the pQCD calculations in [18], which is an extension of the BFKL[19] approach taken in [20, 13]. Both ρ° and ϕ data are well described. This is also true for the heavy quark calculation of [13], shown for the J/Ψ data in Fig.6c.

Helicity studies: The angular distributions involved in the production and decay of the vector mesons V in the reaction $\gamma^* p \to V\, p$ provide information about the polarization states of the photon and V. Studies of these angular distributions are particularly interesting at large values of Q^2 and $|t|$, since pQCD models (*e.g.* [21, 22]) make predictions about the polarization in these regimes. Thus dominance is expected of longitudinally polarized vector mesons produced by longitudinally polarized photons and violation of SCHC is also predicted.
Three angles are defined in the helicity system, the commonly used reference frame:

- Φ: in the hadronic (γp) CM the azimuthal angle between the electron scattering plane and the plane containing V and the scattered proton,
- θ^*: the decay angle of the 2-body decay of V, defined by the positive decay particle in the rest system of V, with the quantization axis taken as the direction of V in the γp CM,
- φ: the azimuthal angle of the positive decay particle in the rest system of V, *i.e.* the angle between the V decay and the V production planes.

The normalized angular distribution $W(\cos\theta^*, \varphi, \Phi)$ can be written [23] as a function of 15 quantities $r_{ik}^{\alpha}, r_{ik}^{04}$, which are linear combinations of the spin density matrix elements (SDMEs). The subscripts i and k take the values of the possible helicity states $-1, 0, 1$. The superscripts 0 and 4 refer respectively to unpolarized transverse photons and longitudinally polarized photons, superscripts $\alpha = 1$ and 2 correspond to linearly polarized transverse photons, and superscripts $\alpha = 5$ and 6 represent the interference of transverse and longitudinal amplitudes.
In the case of SCHC and natural parity exchange (NPE) the 15 independent SDMEs are constrained, and only 5 elements are non-zero.

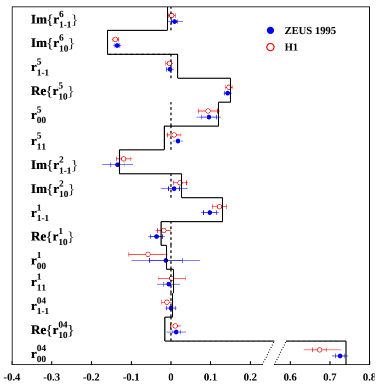

Figure 7: 15 SDMEs from exclusive ρ° electroproduction data. Full and dotted lines: pQCD calculation[22] and SCHC expectation.

H1 and ZEUS have performed large statistics helicity analyses of elastic ρ° [24] and ϕ [25] electroproduction. The result for the ρ° analysis is shown for the two experiments in Fig. 7, where all 15 SDMEs have been determined. The prediction from SCHC and NPE is shown as dotted lines at zero. The two experiments (which are in very good agreement with each other) deviate significantly from this prediction in one element, namely r_{00}^5 which is clearly non-zero. This deviation is predicted by the pQCD model of Ivanov and Kirschner [22], which is everywhere in excellent agreement with the data. The element r_{00}^5 is approximately proportional to the amplitude T_{01} for a transverse photon to produce a longitudinal vector meson.

Recently, H1 and ZEUS have extended the helicity studies of ρ° production to larger values of Q^2 and $|t|$[6, 16, 26]. The H1 analysis studies the single angular distributions

$$W(\Phi) \propto \; 1 - \epsilon \cos 2\Phi (2r_{11}^1 + r_{00}^1) + \sqrt{2\epsilon(1+\epsilon)} \cos\Phi (2r_{11}^5 + r_{00}^5) \qquad (3)$$

and

$$W(\cos\theta^*) \;\sim\; 1 - r^{04}_{00} \;+\; (3\,r^{04}_{00} - 1)\cos^2\theta^* \tag{4}$$

in each of which the two remaining angles have been integrated over. The polarization parameter ϵ has the value ≈ 0.99 in these analyses.

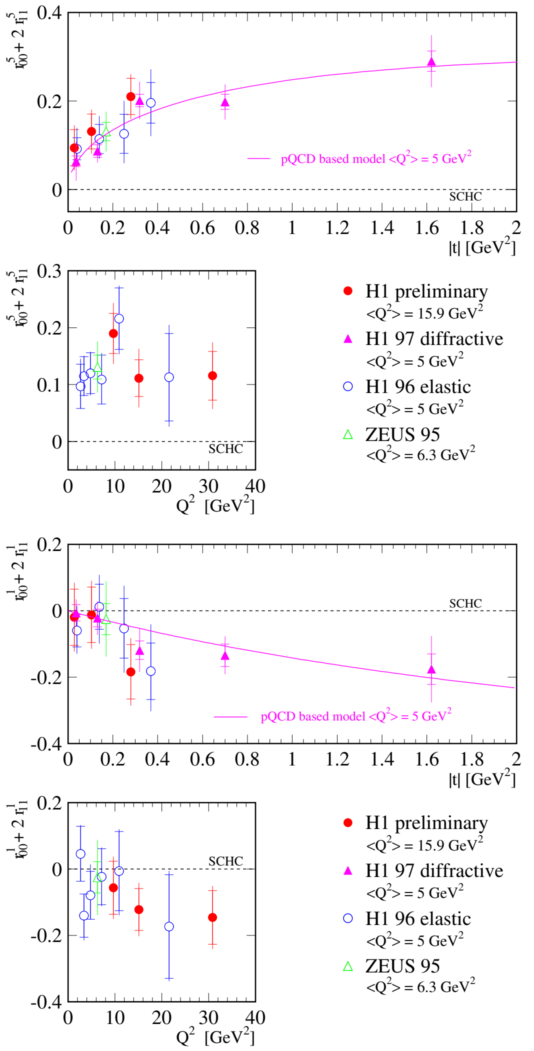

Figure 8: Exclusive ρ° production. $|t|$ and Q^2-dependence of the SDME combination $r^5_{00} + 2r^5_{11}$ (top) and $r^1_{00} + 2r^1_{11}$ (bottom). The curves show a pQCD model[22], the dotted lines give the SCHC expectation.

Fig. 8 shows the determination of the SDME combinations $r^5_{00} + 2r^5_{11}$ and $r^1_{00} + 2r^1_{11}$, as functions of $|t|$ and Q^2. In the former combination the element r^5_{00} dominates. As seen, the previously observed significant SCHC violation in this element persists at high values of $|t|$ and Q^2, and is increasing with $|t|$. The $\sim\sqrt{|t|}$ behaviour, which is predicted by pQCD for the combination $r^5_{00} + 2r^5_{11}$, describes the data well.

In the second combination the element r^1_{00} dominates. At large values of $|t|$ and Q^2 significant SCHC violation is observed. Also r^1_{00} corresponds to the probability for a transverse photon to produce a longitudinal vector meson. Data are consistent with the predicted $\sim$linear $|t|$-dependence. Note that a significant non-zero value for r^1_{00} is not seen in the earlier studies (Fig. 7) at low $|t|$ and moderate Q^2 values.

The determination of the element r^{04}_{00} from the angular distribution (4) is shown in Fig. 9, as function of $|t|$ and Q^2. The $|t|$-dependence is constant, as predicted in pQCD. Note that data from two different Q^2 ranges are shown; r^{04}_{00} is strongly increasing with Q^2.

The element r_{00}^{04} represents the probability to produce a longitudinal vector meson, from either a transverse or a longitudinal photon. It can be directly related to the ratio $R = \sigma_L/\sigma_T = 1/\epsilon \cdot r_{00}^{04}/(1-r_{00}^{04})$. This relation is valid in the SCHC approximation, i.e. if SCHC is assumed (in view of the previous findings, this is not quite correct and leads to a few % overestimate in R). The R values determined from r_{00}^{04} are shown in Fig. 10 as a function of Q^2 and are well described by a pQCD calculation[27]. For details of the deviation from the naively expected linear Q^2 dependence, see [27].

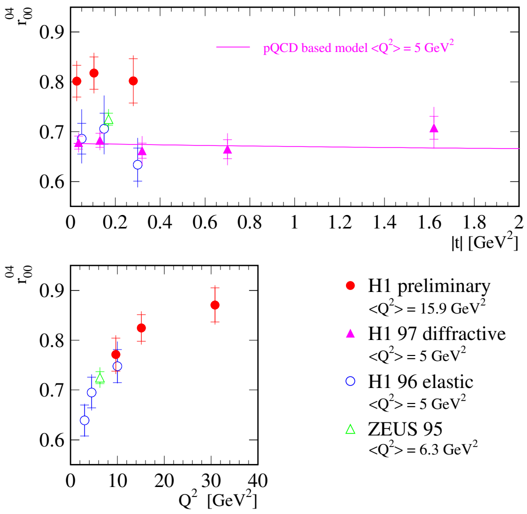

Figure 9: $|t|$ and Q^2-dependence of the SDME r_{00}^{04} in exclusive ρ° production. The curve shows the pQCD model [22] prediction for the lower Q^2 range.

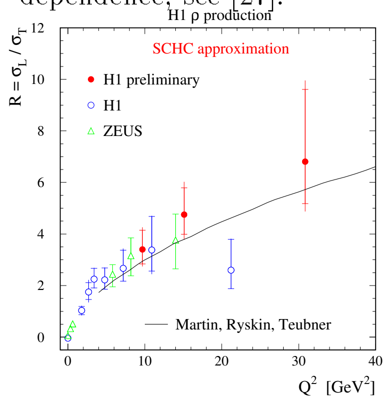

Figure 10: Exclusive ρ° production. Q^2 dependence of the ratio $R = \sigma_L/\sigma_T$ in the SCHC approximation. The curve shows the pQCD model of [27].

The examples given above have amply demonstrated that the quark mass, as well as Q^2 and t all can serve as a hard scale in pQCD calculations. The pQCD approach gives a successful description of exclusive vector meson production at large values of these scales, where the traditional "soft" approach, using VDM and Regge theory, fails. It should however be remembered that the HERA data not only confirm pQCD calculations, but also inspire further development of the theory, in particular where the data are NOT described; a recent example is given in [16], where the helicity structure of high $|t|$ photoproduction data is not reproduced by any of the available pQCD models.

The coverage of the transition region in all involved scales makes HERA an ideal place for these studies. Much enlarged statistics for further advances in this field will soon be available, both in the remaining, still to be analyzed, HERA-I data, and from the coming years of high luminosity running at the upgraded HERA-II. In particular it will then be interesting to see global analyses, using exclusive vector meson production data in combination with inclusive measurement results, like structure functions, jet analyses and inclusive charm production. Such global analyses should yield the ultimate reachable precision and consistency in the parton densities and in the pQCD description of the various reactions, and eventually lead to a deeper understanding of the nature of diffraction.

3. Search for Odderon Exchange

The developments in QCD in the last 20 years have led to the understanding of Pomeron exchange as an exchange of two gluons, the simplest system for exchanging the quantum numbers of the vacuum. Similarly, the exchange of three gluons, also called Odderon exchange, is now recognized as an important and basic prediction of pQCD. After the early seminal papers [28] established the Odderon as the $C = P = -1$ "partner" of the Pomeron, several authors have suggested suitable reactions for its discovery, based upon asymmetries due to Pomeron-Odderon interference[29], or exploiting the specific quantum numbers of the Odderon exchange in exclusive production processes. However, cross sections calculated in pQCD for such exclusive production are in general very small[30] and hardly accessible even with the HERA-II data.

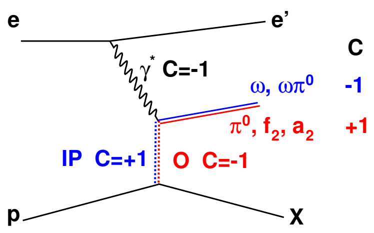

Figure 11: Odderon-photon (Pomeron-photon) fusion, leading to C-parity +1 (−1) exclusive final states.

Recently, large cross sections for Odderon exchange in soft, exclusive photoproduction processes have been predicted[31], using a non-perturbative QCD approach based on the Stochastic Vacuum Model (SVM)[32]. This model is very successful in describing a variety of data[33], also data from HERA. Its extension, including Odderon exchange in which the proton (a quark-diquark system in the model) is excited into a $P = -1$ N^* state, leads to predictions for the exclusive photoproduction of pseudoscalars and tensor mesons, reactions to which Pomeron exchange cannot contribute. The predicted cross sections are large enough to be seen at HERA, and H1 have made a search for such reactions.

The difference between Pomeron and Odderon exchange is obvious in the diagram of Fig. 11. While Pomeron exchange results in $C = -1$ final states, Odderon exchange leads to $C = +1$ final states. Multi-photon exclusive final states can then easily be separated into the two classes: even number of photons have $C = +1$ (Odderon exchange), odd number of photons $C = -1$ (Pomeron exchange). Candidate multi-photon final states are e.g. $\pi^\circ \rightarrow$

2γ, $f_2(1270) \to \pi^\circ\pi^\circ \to 4\gamma$ and $a_2(1320) \to \pi^\circ\eta \to 4\gamma$, all with $C = +1$, and $\omega \to \gamma\pi^\circ \to 3\gamma$ and $b_1(1235) \to \omega\pi^\circ \to 5\gamma$, both with $C = -1$.

The photons were detected in the backward calorimeters of H1 and the scattered electron in the small angle electron tagger (tagged photoproduction). The 3γ mass spectrum[34] for the exclusive three-photon sample is shown in Fig. 12. Only events which are candidates for the final state $\gamma\pi^\circ$ are included. A clear ω peak is seen above the background. The preliminary cross section (at $W_{\gamma p} \approx 200$ Gev), $\sigma(\gamma p \to \omega p) = (1.25 \pm 0.17 \pm 0.22)$ μb agrees very well with the expectation from the W^δ dependence for ω photoproduction (see Fig.2).

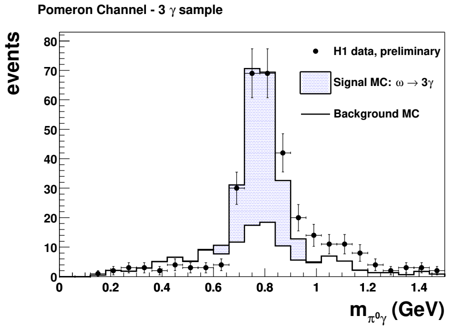

Figure 12: Three photon invariant mass, for $\gamma\pi^\circ$ event candidates. Model prediction and expected background (hatched and white histograms) are also shown.

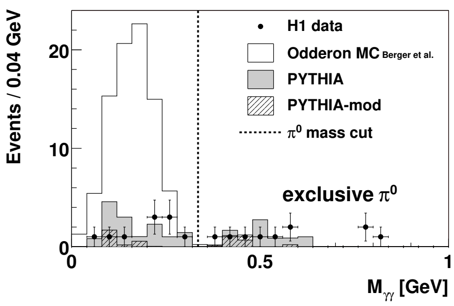

Figure 13: Two photon invariant mass, for exclusive two photon event candidates. The expectations from background and model are shown as hatched and white histograms.

The measurements in the 3-photon and and also 5-photon final states ($\gamma p \to \omega\pi^\circ X$, not discussed here) are interesting in themselves, but for the present purpose can be taken as proof that the photon and π° detection with the H1 detector is well understood. Turning now to the $C = +1$ multi-photon final states, the 2γ mass spectrum of exclusive two-photon events[35] is shown in Fig. 13. Only very few events are seen, compatible with the expected background, and there is no indication of a π° peak. This is in stark contrast to the expectation from the model prediction, > 100 events. Taking all events below the generous π° mass cut as signal events, the upper limit $\sigma(\gamma p \xrightarrow{\mathbb{O}} \pi^\circ N^*) < 49$ nb (95% CL)
is derived, for $< W >= 215$ GeV and the range $0.02 < |t| < 0.3$ GeV^2 covered by the experiment. The limit is clearly below the predicted cross section of > 200 nb. Note that the limit is given for the N^* final state, since in this case a neutron from the N^* decay was detected and used in the trigger.

4γ mass distributions[34] are shown for $\pi^\circ\pi^\circ$ and $\pi^\circ\eta$ final state candidate events in Figs.14a and 14b, respectively[34]. Again, the data are consistent with the expected background, and lie below the model prediction for exclusive $f_2(1270)$ and $a_2(1320)$ resonance production via Odderon exchange. The (still preliminary) upper limits are in these cases (95 % CL)

$$\sigma(\gamma p \xrightarrow{\mathbb{O}} f_2(1270)X) < 16 \text{ nb} \quad \text{and} \quad \sigma(\gamma p \xrightarrow{\mathbb{O}} a_2(1320)X) < 96 \text{ nb},$$

to be compared to the model predictions of 21 and 190 nb, respectively.

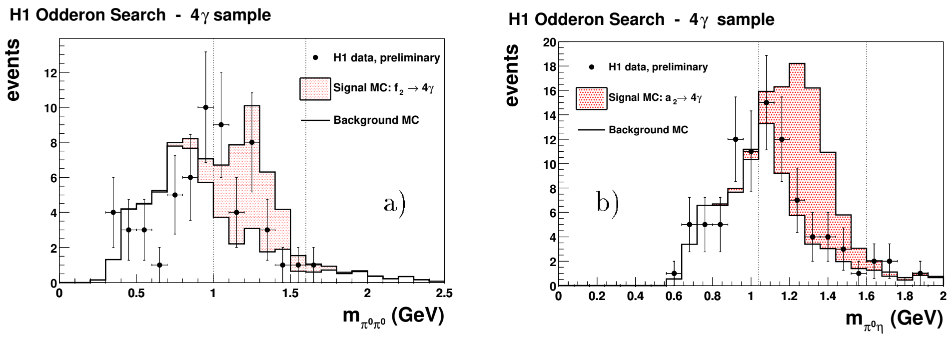

Figure 14: Four photon invariant mass, for a) $\pi^\circ\pi^\circ$ and b) $\pi^\circ\eta$ event candidates. Also shown are the expectations from model and background (hatched and white histograms). Vertical lines indicate the f_2 and a_2 mass regions for the upper limits derivation.

Thus, no evidence of Odderon exchange was found at the cross section levels predicted by the Stochastic Vacuum Model. This result is currently not understood. A possible explanation could be that the Odderon intercept $\alpha_{\mathbb{O}}$ is much smaller than unity; the SVM predictions are made for $W = 20$ GeV and $\alpha_{\mathbb{O}} \gtrsim 1$. Indeed, $\alpha_{\mathbb{O}} < 0.7$ is compatible with the upper limit for exclusive π° photoproduction and also with alternative predictions[36].
Nevertheless, the search at HERA for the Odderon will be continued, both with higher statistics for the above reactions (noting that the upper limit for $f_2(1270)$ production is just below the model prediction), and in other final states where *e.g.* predictions of asymmetry due to Pomeron-Odderon interference[29] can be tested.

4. Open Charm Spectroscopy

The study of inclusive heavy quark production at HERA has many facets, see *e.g.* the extensive review in [37]. In LO QCD, charm quarks are produced via the Boson-Gluon-Fusion (BGF) diagram in Fig. 15a. The photon interacts pointlike. Taking photon structure into account ("resolved" photon), the diagrams in Figs. 15b and 15c contribute, with either a gluon or a c quark interacting with the gluon from the proton structure. In the latter case ("charm excitation") the photon remnant will also contain a charm quark. Thus, charm production gives access both to the gluon density of the proton (direct sensitivity via BGF) and to the charm content (charm structure function) of the proton and photon. The c quark mass together with Q^2 provide hard scales for pQCD calculations of charm production, and the HERA data are used to test these calculations.

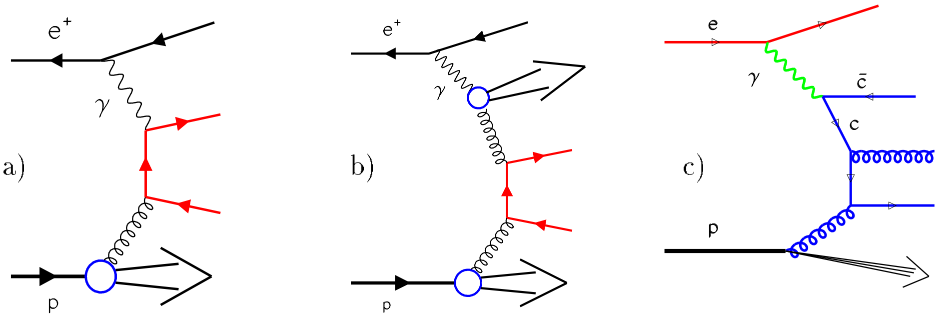

Figure 15: Diagrams contributing to charm production in LO QCD. a) boson-gluon fusion, b) and c) resolved photon interactions.

However, the fragmentation of the charm quarks, once produced, cannot be predicted in pQCD. Non-perturbative, empirical models of the charm fragmentation can be tuned with the measurements at HERA and elsewhere, and by comparison of HERA ep data with data from e^+e^-, $\gamma\gamma$ and $p\bar{p}$ collisions the principle of universality of charm fragmentation can be tested. Thus, charm spectroscopy is an important aspect of heavy quark physics at HERA; here, some recent results from the H1 and ZEUS measurements of D-meson production are presented.

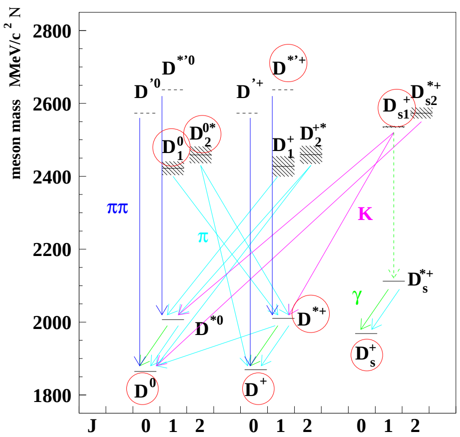

Figure 16: D-meson spectroscopy. The rings indicate the states studied so far by H1 and ZEUS.

The spectroscopy of D-mesons is shown in Fig.16. The states which are ringed have so far been addressed in the HERA studies. The access to these states is so far limited to decay modes into final states consisting of charged particles only. They include the $L = 0$ states, namely the pseudoscalar D-mesons and the vector D^*-mesons, as well as the heavier P-wave states. A search has also been made for radially excited D^*-states.

The experimental detection is based on two different techniques, either a lifetime measurement, using a high precision vertex detector to locate the charmed meson decay vertex, or the well-known Δm technique, utilizing the limited phasespace (mass difference $\sim$ 10 MeV) for the decay $D^*(2010) \rightarrow D\pi_s$, where π_s is a "slow" pion.

***D*-meson production cross sections:** New measurements of the production cross sections for all pseudoscalar D-mesons (the data are shown in Fig. 17), as well as for the $D^*(2010)$, are available from H1[38]. They are based on the H1 silicon vertex detector (CST) data and the D^+ measurement[1] is the first at HERA.

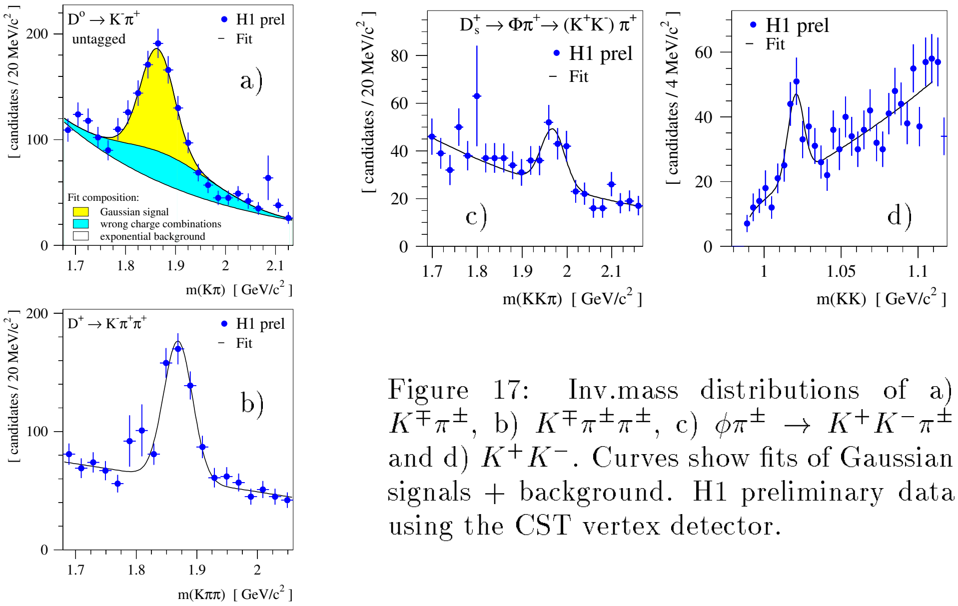

Figure 17: Inv.mass distributions of a) $K^{\mp}\pi^{\pm}$, b) $K^{\mp}\pi^{\pm}\pi^{\pm}$, c) $\phi\pi^{\pm} \rightarrow K^+K^-\pi^{\pm}$ and d) K^+K^-. Curves show fits of Gaussian signals + background. H1 preliminary data using the CST vertex detector.

H1	Visible Cross Section (nb)	
Prel.	Measurement	LO QCD
D^+	$2.16 \pm 0.19 \, ^{+0.46}_{-0.35}$	2.45 ± 0.30
D°	$6.53 \pm 0.49 \, ^{+1.06}_{-1.30}$	5.54 ± 0.69
D_s^+	$1.67 \pm 0.41 \, ^{+0.54}_{-0.54}$	1.15 ± 0.30
D^{*+}	$2.90 \pm 0.20 \, ^{+0.58}_{-0.44}$	2.61 ± 0.31

Table 1: Visible cross sections for D-meson production, compared to the LO QCD (AROMA 2.2) prediction.

The measured visible cross sections are given in Table 1. The kinematic range of the measurements is

$2 < Q^2 < 100$ GeV^2,
$0.05 < y < 0.7$,
$p_\perp(D) > 2.5$ GeV and
$|\eta(D)| < 1.5$,

where y is the inelasticity and η the pseudo-rapidity.

The cross sections in Table 1 are compared to the Leading Order (LO) QCD prediction, obtained with the Monte Carlo (MC) generator program AROMA 2.2[39]. Good agreement with the data is observed. Note that

[1] The charge conjugate states are always implicitly included.

both the measured and the predicted cross sections include contributions from decays of b flavoured hadrons into D-mesons. These contributions are taken from the AROMA simulation and the cross section measurements are converted into fragmentation factors $f(c \to D)$, using the expression

$$f(c \to D) = \frac{\sigma_{vis}^{meas}(ep \to eDX) - \sigma_{vis}^{MC}(ep \to b\bar{b} \to eDX)}{\sigma_{vis}^{MC}(ep \to c\bar{c} \to eDX)} \cdot f_{w.a.}(c \to D),$$

where the fragmentation dependence $f_{w.a.}$ (the world averages of the charm fragmentation factors are used in the hadronisation part of the MC simulation) has been removed. The resulting measured fragmentation factors are given in Table 2 and compare well with the world average values[40], which are dominated by the LEP e^+e^- results.

H1	Fragmentation Factor	
Prel.	Measurement	World Average
D^+	$0.202 \pm 0.020\ ^{+0.045}_{-0.033}\ ^{+0.029}_{-0.021}$	0.232 ± 0.018
D°	$0.658 \pm 0.054\ ^{+0.115}_{-0.148}\ ^{+0.086}_{-0.048}$	0.549 ± 0.026
D_s^+	$0.156 \pm 0.043\ ^{+0.036}_{-0.035}\ ^{+0.050}_{-0.046}$	0.101 ± 0.027
D^{*+}	$0.263 \pm 0.019\ ^{+0.056}_{-0.042}\ ^{+0.031}_{-0.022}$	0.235 ± 0.010

Table 2: Measured charm fragmentation factors compared with the world average values[40].

Since the cross section measurements are all made in the same kinematic range, ratios of the fragmentation factors can be used to calculate several interesting quantities, characterizing the fragmentation. Thus the fraction of vector mesons P_V produced in the fragmentation, the ratio $R_{u/d}$ of u and d quarks participating in the charm fragmentation, and the strangeness suppression factor γ_s are given by the following expressions, where VM and PS stand for the number of vector mesons and pseudoscalar mesons, and BR are branching ratios:

$$P_V = \frac{VM}{PS + VM} = \frac{f(c \to D^{*+})}{f(c \to D^+) + f(c \to D^{*+})\ BR(D^{*+} \to D^\circ \pi^+)}$$

$$P'_V = \frac{2\ f(c \to D^{*+})}{f(c \to D^+) + f(c \to D^\circ)} \qquad \gamma_s = \frac{2\ f(c \to D_s^+)}{f(c \to D^+) + f(c \to D^\circ)}$$

$$R_{u/d} = \frac{f(c \to D^\circ) - f(c \to D^{*+})\ BR(D^{*+} \to D^\circ \pi^+)}{f(c \to D^+) + f(c \to D^{*+})\ BR(D^{*+} \to D^\circ \pi^+)}$$

In the ratio P'_V isospin invariance has been used, i.e. it is assumed that $f(c \to D^{*+}) = f(c \to D^{*\circ})$.

The obtained numbers, $P_V = 0.693 \pm 0.045 \pm 0.004 \pm 0.009$, $R_{u/d} = 1.26 \pm 0.20 \pm 0.13 \pm 0.04$ and $\gamma_s = 0.36 \pm 0.10 \pm 0.01 \pm 0.08$, agree well with the world average values (calculated using [40]) of 0.601 ± 0.032, 1.00 ± 0.09 and 0.26 ± 0.07, respectively. The ZEUS measurements[41] of $\gamma_s = 0.27 \pm$

0.05 ± 0.07 and $P'_V = 0.546 \pm 0.045 \pm 0.028$ also compare well with the world average and with the H1 measurement of $P'_V = 0.613 \pm 0.061 \pm 0.033 \pm 0.008$, respectively.

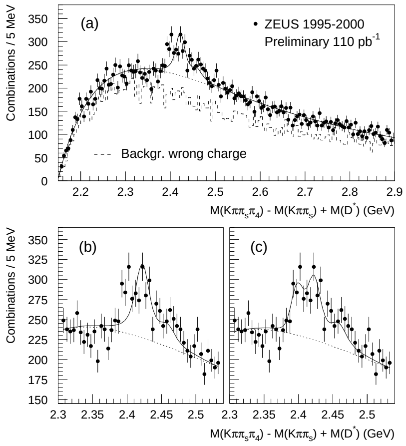

Figure 18: Mass distribution $\Delta M^{**} = M(K\pi\pi_s\pi_4) - M(K\pi\pi_s) + M(D^{*\pm}(2010))$. The fits are described in the text.

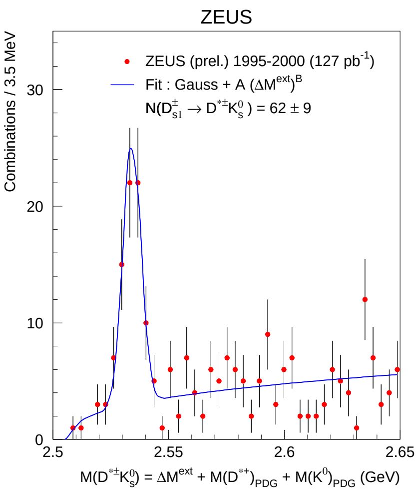

Figure 19: Mass distribution $\Delta M^{ext} = M(K\pi\pi_s\pi_3\pi_4) - M(K\pi\pi_s) - M(\pi_3\pi_4)$

The world average values of these fragmentation sensitive ratios are dominated by the LEP e^+e^- results. Thus one may conclude that the hypothesis of charm fragmentation universality is well supported by the HERA ep data. It is argued in [42] that different processes may be sensitive to different aspects of fragmentation, and that universality may not hold.

Observation of *P*-wave states: ZEUS observe two neutral states, using an "extended Δm" tagging method, in which still another pion with the correct charge was added to the D^* candidate combination[43]. The corresponding mass distribution is shown in Fig. 18. A fit which includes two Breit-Wigner shapes, folded with the resolution and including the expected helicity spectra ($J^P = 1^+$ and 2^+), describes the data (Fig. 18b). The two states agree in mass and width with the $L = 1$ states previously seen in e^+e^- collisions, namely $D_1^\circ(2420)$ and $D_2^{*\circ}(2460)$[44]. The fragmentation factors determined by ZEUS, $f(c \to D_1^\circ) = 1.46 \pm 0.18 \,^{+0.33}_{-0.27} \pm 0.06$ % and $f(c \to D_2^{*\circ}) = 2.00 \pm 0.58 \,^{+1.40}_{-0.48} \pm 0.41$ %, also agree with the previous measurements.

The mass spectrum in Fig. 18 is complicated by the indication of a third mass state, not previously seen. Fig. 18c shows a fit with an added Breit-Wigner shape for a new hypothetical state at $\sim$ 2.4 GeV. Is it an interference effect, a fluctuation, or indeed a new state?

The strange-charmed P-wave state $D^{\pm}_{s1}(2536)$ is also observed by ZEUS[45], in the "extended Δm" distribution $\Delta M^{ext} = M(K\pi\pi_s\pi_3\pi_4) - M(K\pi\pi_s) - M(\pi_3\pi_4)$, in which the two additional pions form a K°_S. The statistics in Fig. 19, 62 ± 9 events, are not enough to establish the spin-parity, decay distributions are compatible both with $1^+, 1^-$ and 2^+.

Nevertheless, both mass and width and the fragmentation factor, $f(c \rightarrow D^{\pm}_{s1}) = 1.24 \pm 0.18 \ ^{+0.08}_{-0.06} \pm 0.14(\mathrm{br.})$ %, are in good agreement with the previous e^+e^- observations[44]. Not understood is the fact that $f(c \rightarrow D^{\pm}_{s1}) > \gamma_s \cdot f(c \rightarrow D^\circ_1)$, meaning that the strangeness suppression, which was determined using the S-wave states, seems not to be valid for this P-wave state.

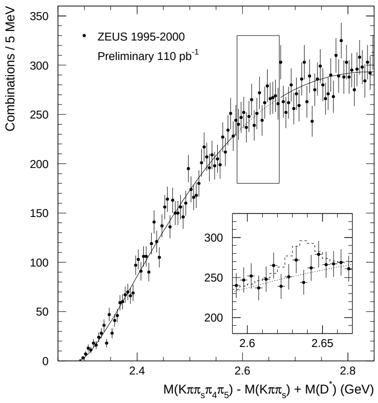

Figure 20: Mass distribution $\Delta M^{*\prime} = M(K\pi\pi_s\pi_4\pi_5) - M(K\pi\pi_s) + M(D^{*\pm})$. The insert shows the signal expectation corresponding to the upper limit.

Finally, ZEUS[43] have also searched for the narrow state seen by DELPHI[46] at 2637 MeV and decaying into $D^{*\pm}\pi^+\pi^-$. At this mass, radially excited D^*-mesons are expected[47]. The search method is again an "extended Δm" combination, $\Delta M^{*\prime} = M(K\pi\pi_s\pi_4\pi_5) - M(K\pi\pi_s) + M(D^{*\pm})$, where two pions $\pi^+\pi^-$ have been added to the $D^{*\pm}$ candidate combinations. The mass spectrum in Fig. 20 shows no significant peak, and an upper limit is set, $R_{D^{*\prime\pm} \rightarrow D^{*\pm}\pi^+\pi^-/D^{*\pm}} < 2.3\%(95\%\ \mathrm{C.L.})$, which contradicts the DELPHI observation. The upper limit can also be expressed as a limit on the corresponding fragmentation factor, $f(c \rightarrow D^{*\prime\pm}) \cdot BR(D^{*\prime +} \rightarrow D^{*+}\pi^+\pi^-) < 0.7$ % (95% C.L.). OPAL and CLEO [48] also could not confirm the DELPHI observation, and OPAL gave the value 0.9 % for this limit.

In conclusion, the Charm Spectroscopy is a very active field in the HERA physics, and it will greatly profit from the HERA-II luminosity upgrade and from the recent H1 and ZEUS detector improvements, in particular in the areas of triggering, tracking and vertex detection.

5. Acknowledgments

It is a pleasure to thank the organizers for the warm and joyful atmosphere in an exciting, interesting and very well prepared conference. I also wish to thank my colleagues in H1 and ZEUS, for providing the data and the results shown in this report and for all their help given to me. I am particularly indebted to L. Gladilin, D. Ozerov and Y. Yamazaki for critical remarks to the manuscript.

REFERENCES

[1] J.A. Crittenden, Springer Tracts in Modern Physics, Volume 140 (Springer, Berlin Heidelberg, 1997)

[2] H. Abramowicz and A. Caldwell, Rev.Mod.Phys.71 (1999) 1275

[3] S.J. Brodsky *et al.*, Phys. Rev. **D50** (1994) 3134

[4] M.G. Ryskin, Z. Phys. **C57** (1993) 89

[5] M. Erdmann, Proceedings ICHEP1998, Vancouver, Canada, Vol. 1, p. 217

[6] H1 Collab., presented by X. Janssen in DIS2002, Kraków, Poland, http://www-h1.desy.de/psfiles/confpap/DIS2002/H1prelim-02-015.ps

[7] A. Donnachie and P.V. Landshoff, Nucl.Phys. **B231** (1984) 189

[8] ZEUS Collab., S. Chekanov *et al.*, Eur.Phys.J. **C24** (2002) 345;
ZEUS Collab., presented by A. Levy in DIS2002, Kraków, Poland;
H1 Collab., C. Adloff *et al.*, Eur.Phys.J. **C10** (1999) 373;
H1 Collab., C. Adloff *et al.*, Phys.Lett **B483** (2000) 23

[9] L. Frankfurt, W. Koepf and M. Strikman, Phys. Rev. **D57** (1998) 512

[10] A.D. Martin, M.G. Ryskin and T. Teubner, Phys. Rev. **D26** (1999) 14022

[11] CTEQ Collab. H.L. Lai *et al.*, Eur.Phys.J. **C12** (2000) 375;
CTEQ Collab. H.L. Lai *et al.*, Phys.Rev.. **D55** (1997) 1280

[12] H1 Collab., presented by D. Brown in DIS2001, Bologna, Italy, http://www-zeus.desy.de/conferences/01/2001_DIS_brown_writeup.ps.gz

[13] J. Bartels *et al.*, Phys.Lett. **B375** (1996) 301

[14] ZEUS Collab., presented by A. Kreisel in DIS2001, Bologna, Italy, http://www-zeus.desy.de/conferences/01/2001_DIS_kreisel.ps.gz

[15] L. Frankfurt, W. Koepf and M. Strikman, Phys. Rev. **D54** (1996) 3194

[16] ZEUS Collab., S. Chekanov *et al.*, Preprint DESY-02-072, hep-ex/0205081

[17] D.Yu. Ivanov *et al.*, Phys.Lett. **B478** (2000) 101; Err. Phys.Lett. **B498** (2001) 295

[18] J.R. Forshaw and G. Poludniowski, Preprint hep-ph/0107068

[19] E.A. Kuraev, L.N. Lipatov and V.S. Fadin, Sov.Phys.JETP **45** (1977) 199;
Ya.Ya. Balitskiĭ and L.N. Lipatov, Sov.J.Nucl.Phys. **28** (1978) 822

[20] J.R. Forshaw and M. Ryskin, Z.Phys. **C68** (1995) 137

[21] I. Royen and J. Cudell, Nucl.Phys. **B5454** (1999) 505;
I. Royen, Phys.Lett. **B513** (2001) 337;
E.A. Kuraev, N.N. Nikolaev and B.G. Zakharov, JETP Lett. **68** (1998) 696

[22] D.Yu.Ivanov and R. Kirschner, Phys. Rev. **D58** (1998) 114026

[23] K. Schilling and G. Wolf, Nucl. Phys. **B61** (1973) 381;
for a detailed discussion, see also [1]

[24] ZEUS Collab., J. Breitweg *et al.*, Eur.Phys.J. **C12** (2000) 393;
H1 Collab., C. Adloff *et al.*, Eur.Phys.J. **C13** (2000) 371

[25] ZEUS Collab., contr. paper 793 to ICHEP 1998, Vancouver, Canada

[26] H1 Collab., C. Adloff *et al.*, Phys.Lett. **B539** (2002) 25

[27] A.D. Martin, M.G. Ryskin and T. Teubner, Phys. Lett. **B454** (1999) 339

[28] L. Łukaszuk and B. Nicolescu, Lett.Nuov.Cim. **8** (1973) 405;
K. Kang and B. Nicolescu, Phys.Rev. **D11** (1975) 2461;
G. Białkowski, K. Kang and B. Nicolescu, Lett.Nuov.Cim. **13** (1975) 401;
D. Joynson *et al.*, Nuov.Cim. **30A** (1975) 345

[29] S.J. Brodsky, J. Rathsman and C. Merino, Phys.Lett. **B461** (1999) 114;
A. Ahmedov *et al.*, Eur.Phys.J. **C11** (1999) 703;
I.P. Ivanov, N.N. Nikolaev and I.F. Ginzburg, hep-ph/0110181;
I.F. Ginzburg, I.P. Ivanov and N.N. Nikolaev, hep-ph/0207345;
Ph. Hägler *et al.*, Phys.Lett. **B535** (2002) 117; Err. Phys.Lett. **B540** (2002) 324;
Ph. Hägler *et al.*, hep-ph/0207224, to be published in Eur.Phys.J.

[30] J. Bartels *et al.*, Eur.Phys.J. **C20** (2001) 323

[31] E.R. Berger *et al.*, Eur.Phys.J. **C9** (1999) 491;
E.R. Berger *et al.*, Eur.Phys.J. **C14** (2000) 673;
H.G. Dosch, private communication, Heidelberg (2001)

[32] H.G. Dosch and Yu. A. Simonov, Phys.Lett. **B205** (1988) 339;
O. Nachtmann, Ann.Phys. **209** (1991) 436

[33] A. Donnachie and H.G. Dosch, Phys.Rev. **D65** (2002) 014019

[34] H1 Collab., contr. paper 795 to IECHEP 2001 Budapest, Hungary

[35] H1 Collab., C. Adloff *et al.*, DESY preprint 02-087, hep-ex/0206073, to be published in Phys.Lett. **B**

[36] A.B. Kaidalov and Yu.A. Simonov, Phys.Lett. B477 (2000) 163

[37] P.J. Bussey, Int.J.Mod.Phys. **A17** (2002) 1065

[38] H1 Collab., presented by J. Wagner in DIS2002, Kraków, Poland,
http://www-h1.desy.de/psfiles/confpap/DIS2002/H1prelim-02-076.ps

[39] G. Ingelman, J. Rathsman and G.A. Schuler, Comput.Phys.Commun. **101** (1997) 135

[40] L. Gladilin, "Charm Hadron Production Fractions", hep-ex/9912064

[41] ZEUS Collab., J. Breitweg *et al.*, Phys.Lett. **B481** (2000) 213;
ZEUS Collab., contr. paper 501 to IECHEP 2001, Budapest, Hungary

[42] S. Frixione *et al.*, J.Phys. **G27** (2001) 27;
P. Nason *et al.*, in LHC workshop on Standard Model Physics, hep-ph/0003142

[43] ZEUS Collab., contr. paper 448 (Abstr. 854) to ICHEP 2000, Osaka, Japan

[44] Particle Data Group, D.E. Groom *et al.*, Eur.Phys.J. **C15** (2000) 1

[45] ZEUS Collab., contr. paper 497 to IECHEP 2001, Budapest, Hungary

[46] DELPHI Collab., P. Abreu *et al.*, Phys.Lett. **B426** (1998) 231

[47] S. Godfrey and N. Isgur, Phys.Rev. **D32** (1985) 189;
D. Ebert *et al.*, Phys.Rev. **D32** (1998) 5663

[48] OPAL Collab, G. Abbiendi *et al.*, Eur.Phys.J. **C20** (2001) 445;
CLEO Collab., presented by J.L. Rodriguez in HQ98, hep-ex/9901008